TRANSPORT THEORIES APPLIED TO THE STUDY OF CONVOY ELECTRON PRODUCTION

M.L.Martiarena and C.R.Garibotti

Centro Atómico Bariloche - 8400 Bariloche - Argentina - CONICET

ABSTRACT

We write a transport equation for the electrons produced when atomic or ionic beams travers a foil. We consider that the electrons are produced inside the solid by the electron loss and capture to continumm mechanisms. They lost energy by inelastic collisions with the target atoms and are deflected by elastic scattering. We study the electron distribution for H^0 and H^+ projectiles on carbon foils for differents thicknesses. We obtain a description of the electron velocity spectra in the forward direction which agrees with the experiments. Studying the ratio between the intrinsic convoy electron height and the not convoy electron or "background" intensity, at convoy electron velocity, we obtain a constant behaviour for different target thicknesses.

PACS numbers: 34.10.+X ; 79.20-m

INTRODUCTION

In the electron spectrum resulting from ion-solid-foil collision a sharp peak is observed in the forward direction centered at the same velocity as the emergent ion. These electrons which go away with the ion are called "convoy electrons". The origin of that process is an interesting subject of discussion and several models have been proposed[1]. Dettmann et al[2] consider a single collision model where the ion captures one electron into a continuum state (ECC) in the last layer of the foil. This is only qualitatively true, for sufficiently fast protons and thin targets. As a foil never presents a thin target, the electron loss to continuum (ELC) must be considered as a competing process[3]. This ELC process will be effective even for bare incident projectiles.

A completely different model for the production of convoy-foil electrons considers collective properties of the valence-electron plasma in a solid[4]. If the projectile velocity is greater than the Fermi velocity v_F, it is possible that a perturbation of the plasma density stays behind the ion. This perturbation consists of an alternately enhanced and depleted electron density relative to the mean density in the medium, creating regions of negative and positive potential. This wake accompanies the ionic projectile and can trap the electrons into bound states. The production of convoy electrons originating from this "wake-riding" model can be considered as a special case of ELC[3].

The shapes and intensities of convoy-electron spectra as a function of projectiles species, energies, and electron ejection angles have been extensively studied experimentally, for foil target thick enough to attain projectile charge equilibrium[5]. Recently, experiments have been made to study the convoy-electron production when the charge state of the emergent beam is out of equilibrium[6-11]. The typical convoy cusp is observed at the ion velocity when bare ions interact with thin target foils, which almost no changes with increasing foil thickness. When the projectil bears bound electrons an additional peak appears for intermediate foil thicknesses, which broadens and is shifted to low velocities for increasing thickness, as shown in Fig. 1.

Some models have been proposed to describe the two observed features. Yamazaki and Oda[12] consider that the electrons loose their correlation to the moving beam in the solid by collisions. Part of these electrons emerge from the surface with a velocity distribution centered in the zero velocity peak, constituting a background spectrum. The ions in the beam capture electrons from this distribution to produce the convoy peak. They found that the ratio between this "intrinsic" convoy electron peak height to the background yield, for $v = v_1$, is almost independent of the target thickness, as shown in Fig.2b. Barrachina et al[13] assume that convoy electrons are produced inside the target by the ELC process and suffer elastic and inelastic collisions with the atoms before exit. This give a general description of the forward spectrum but does not gives a constant ratio between convoy and background electrons as obtained by Yamazaki and Oda.

In this paper we introduce a transport theory for the problem. We consider that the ion - solid - foil interaction can be modelated as a beam which collides with a gas medium. The transport equation that we study is obtained starting from the Boltzmann equation for several species with creation and removal events[14].

We analyse the allowed channels in the beam-gas collision and introduce some simplifyng assumptions. The electrons are supposed to be produced by ELC and ECC inside the medium and are scattered and lost energy by elastic and excitation collision with the atoms of the medium.

Transport equation for the distributions functions

We consider a mixed beam of atoms and ions which collide with a medium of atoms at rest. We will consider the stationary regime. The Boltzmann equation describing the evolution of the distribution function of each species i, without external forces, is:

$$v.\nabla f_i = \sum_{j=1}^{L} B[f_i, f_j] \qquad (1)$$

with:

$$B[f_i, f_j] = \int dw\, dv'dw'\; W(v\,, w\,|v', w') \qquad (2)$$

$$[f_i(v',x,t)\, f_j(w',x,t) - f_i(v,x\,,t)\, f_j(w,x\,,t)] + \text{Sources}$$

where L is the number of species, $W_h(v,w|v',w')$ is the transition probability for the h reaction channel, which can be expresed in terms of the corresponding differential cross section $\frac{d\sigma(g,g.g')}{dv}$, v and w are the velocities before collision and v' and $\mathbf{w}'$ those after collision. The $\mathbf{v}$, $\mathbf{w}$, $\mathbf{v}'$ and $\mathbf{w}'$ are connected by the laws of conservation of momentum and energy. We call $\mathbf{g} = \mathbf{v} - M\,\mathbf{w}$ and $\mathbf{g}' = \mathbf{v}' - M\,\mathbf{w}'$ the relative velocity of particles.

We will neglect the interactions with the free electrons in the host medium and we assume that the involved species are: ions (I) and atoms that travel with the beam (A), electrons (e) and atoms at rest (B)

The possible collisions channels are:

a) $I + B \longrightarrow I + B$ elastic difussion (σ^{el})

b) $I + B \longrightarrow I + B^{+} + e$ ionization (σ^{i})

c) $I + B \longrightarrow A + B^{+}$ electron capture (σ^{r})

d) $I + B \longrightarrow I + B^{*}$ excitation (σ^{*}_{if})

e) $A + B \longrightarrow A + B$ elastic difussion (σ^{ea})

f) $A + B \longrightarrow A + B^{+} + e$ ionization (σ^{ia})

g) $A + B \longrightarrow A + B^{*}$ excitation (σ^{*a}_{if})

h) $A + B \longrightarrow I + B + e$ electron loss (σ^{el})

i) $e + B \longrightarrow e + B$ elastic difussion (σ^{ee})

j) $e + B \longrightarrow e + B^{*}$ excitation (σ^{*e}_{if})

k) $e + B \longrightarrow e + B^{+} + e$ ionization (σ^{ie})

We assume that the convoy electrons are produced inside the solid, when the ions and atoms in the beam collide with the target atoms at rest, by electron loss and capture to continuum processes. These convoy electrons act as a beam of electrons inside the solid and modify their velocity in magnitude and direction by inelastic and elastic collisions with target atoms.

The evolution equation for the distribution function of the electrons is:

$$v_x \frac{\partial f_e}{\partial x} = H(\mathbf{v},x) - P(\mathbf{v},x)\ f_e(\mathbf{v},x) + G(\mathbf{v},x) \qquad (3)$$

The function $H(\mathbf{v},x)$ represents the electron source:

$$H(\mathbf{v},x) = n_I\ n_B \frac{d\sigma^i}{d\mathbf{v}} + n_A\ n_B \frac{d\sigma^{el}}{d\mathbf{v}} \qquad (4)$$

$\mathbf{v}_1$ is the beam velocity, n_A and n_I are the charge fractions of the neutral atoms and ions in the beam respectively; n_B is the density of atoms at rest in the target. The differential cross sections correspond to the emission of an electron of velocity $\mathbf{v}$ in the collision of a beam particle of velocity $\mathbf{v}_1$ with an atom at rest.

If we analyze the collision between the electron and the target atoms, the conservation equation of momentum and energy are:

$$\mathbf{v}' + M\ \mathbf{w}' = \mathbf{v} + M\ \mathbf{w} \qquad (5)$$

$$v'^2 + M\ w'^2 + 2\ E_i = v^2 + M\ w^2 + 2\ E_{fh} \qquad (6)$$

M is the target mass, E_i and E_{fh} are the electronic energies in the initial state and the excited final state h respectively. We use atomic units.

The function $P(\mathbf{v},x)$ accounts for the loss of electrons of velocity $\mathbf{v}$ by elastic and inelastic collisions between electrons and target atoms at rest. It is:

$$P(\mathbf{v}) = n_B \int [W^{ee}(\mathbf{v},\mathbf{w}|\mathbf{v}',\mathbf{w}') +$$

$$\sum_f W^{if}(\mathbf{v},\mathbf{w}|\mathbf{v}',\mathbf{w}')]\ \delta(\mathbf{w})\ d\mathbf{w}\ d\mathbf{v}'\ d\mathbf{w}' \qquad (7)$$

with:

$$W^{ee}(v\ ,w\ |v',w') = g\ \frac{d\sigma^{ee}(g,g.g')}{dv'}\ \delta(v'+ Mw' - (v\ + Mw\ ))\ \times$$

$$\times\ \delta(v'^2+ Mw'^2-(v^2+ Mw^2)) \qquad (8)$$

and:

$$W^{if}(v\ ,w\ |v',w') = g\ \frac{d\sigma^{*e}_{if}(g,g.g')}{dv'}\ \delta(v'+ Mw' - (v\ + Mw\ ))\ \times$$

$$\times\ \delta(v'^2+ Mw'^2-(v^2+ Mw^2+ \Delta E_{if})) \qquad (9)$$

ΔE_{if} is the energy difference between the final f to initial i state, and $\frac{d\sigma^{*e}_{if}(g,g.g')}{dv'}$ is the differential cross section for inelastic processes including excitation and ionization of target atoms by electronic impact.

The function $G(v,x)$ considers the gain of electrons of velocity v, produced by the above mentioned processes, and is:

$$G(v,x) = G^i+ \sum_f G^{if} \qquad (10)$$

G^{if} are the inelastic gains:

$$G^{if} = n_B \int f_e(v',x)\ \delta(w')\ W^{if}(v\ ,w\ |v',w')\ dw\ dv'dw' \qquad (11)$$

G^e is the elastic one:

$$G^e = n_B \int f_e(v',x)\ \delta(w')\ W^e(v\ ,w\ |v',w')\ dw\ dv'dw' \qquad (12)$$

We define the espatial variable $x' = n_B\ x$. From now on we note $x' \longrightarrow x$.

The functional form of n_A has been obtained by Allison[15]:

$$n_A(x) = n_A(\infty)\ (1 - e^{-\frac{(\sigma^{el} + \sigma^{r})\ x}{v_i}}) + n_A(0)\ e^{-\frac{(\sigma^{el} + \sigma^{r})}{v_i}} \qquad (13)$$

where:

$$n_A(\infty) = \sigma^{r}/(\sigma^{r}+\sigma^{el})\ n_H$$

$$n_I(x) = n_H - n_A(x) \qquad (14)$$

These can be obtanied from an equation similar to Eq.(4), where only the capture and electron loss channels are included.

The equations (3), (4), (7) and (10) determine the spatial evolution of the distribution function. These equations are similar to those in beam slow down, the main difference is the source term.

Here we analyze the simplest model which can describe the experimental data considering the excitation channel alone. A better quantitative and realistic description could be obtained by introduccing the ionization and additional reaction channels. However the required basic information is scarse and therefore these processes will not be considered in the present paper.

We consider that the excitation cross section mainly contributes for small dispersion angles[16] and we do not take into account the atomic recoil. The final form of $G^{i}(v,x)$ is:

$$G^{if}(v,x) = \sum_{f} f_e((v^2+ 2\ \Delta E_{fi})^{1/2}, \vartheta, x) \times$$
$$(v^2+ 2\ \Delta E_{fi})^{1/2}\ \sigma^{*e}_{if}((v^2+ 2\ \Delta E_{fi})^{1/2}) \qquad (15)$$

σ^{*e}_{if} is the total excitation cross section from the initial state i to a final state f.

The electron velocities are within 7 a.u. $\leq$ v $\leq$ 11 a.u. The excitation energy steps for the outer electrons of C atoms are $\Delta E_{fi} \leq 0.4$ a.u. In that case we can consider that $(v^2 + 2\Delta E_{fi})^{1/2} \cong v + \Delta E_{fi}/v$.

The inelastic loss term may be calculated from (7) and (9), resulting:

$$P^i(v,) = v \sum_f \sigma^{*e}_{if}(v) \tag{16}$$

If we consider the conservation of momentum and energy equation, the elastic gain term is:

$$G^e(v,x) = v \int f_e(v,\Omega',x) \frac{d\sigma^{ee}}{d\Omega'}(v,\Omega,\Omega')d\Omega' \tag{17}$$

Ω' and Ω are the directions of electron motion before and after the collision, respectively.

Assuming that the atoms are initially at the ground state i=0 the approximate equation for the evolution of the electronic distribution function now reads:

$$v_x \frac{\partial f_e}{\partial x} = H(v,x) - f_e(v,x)\, v \left(\sum_f \sigma^{*e}_{0f}(v) + \sigma^{ee}(v)\right) + \tag{18}$$

$$+\sum_f f_e((v^2 + 2\ \Delta E_{f0})^{1/2}, \vartheta, x)\ \sigma^{*e}_{0f}((v^2 + 2\ \Delta E_{f0})^{1/2})\ (v^2 + 2\ \Delta E_{f0})^{1/2}$$

$$+ v \int f_e(v,\Omega',x) \frac{d\sigma^{ee}}{d\Omega'}(v,\Omega,\Omega')d\Omega'$$

RESULTS

We will compare our model with the experimental data for electron production by a beam of H^0 and H^+ at 3 MeV colliding with carbon foils. A numerical study of (18) requires the elastic and inelastic cross sections.

The differential elastic cross section are[17]:

$$\frac{d\sigma^{ee}}{d\Omega} \propto Z_p^2/(v^4(\text{sen}^2(\theta/2)+\nu^2)^2) \tag{19}$$

the screening ν is determined by the Thomas-Fermi model, $d\Omega$ is the differential of solid angle and Z_p the projectil charge. The total elastic cross section, calculated using the Thomas-Fermi method is[17]:

$$\sigma^{ee} \propto Z^{4/3}/\ v^2 \tag{20}$$

The total excitation cross section for high energy electron collision in the Bethe[18] description is:

$$\sigma^{ee}_{0f} = (a_f \ \ln E + b_f)/E \tag{21}$$

a_f and b_f are related with the oscillator strength, and for optically forbidden transitions $a_f = 0$.

Lacking experimental data for the excitations of C atoms by electron impact, we consider the theoretical results obtained by P. Ganas[19] for the transitions 2p - ns, 2p - nd and the optical 2p - np, when collision electron incident energies are smaller than 5 Kev. We do a Fano plot from the curves describe by Ganas and by a least square fit we obtain for each transition, the a_f and b_f values. These values are:

2p -	a_f	b_f	ΔE_{f1} [a.u.]
4s	.127	.219	.3559
5s	3.63E-2	9.15E-2	.3822
3p	0.0	3.2	.3370
4p	0.0	.852	.3705
3d	1.114	.234	.3614
4d	.525	2.25E-2	.3832
5d	.235	.164	.3941

In the source term H(v,x) (4), we propose that the ionization ($\frac{d\sigma^{i}}{dv}$) and the electron loss ($\frac{d\sigma^{elc}}{dv}$) differential cross sections, are mainly determined by the Coulomb factor f_c and the soft electron peak. We will assume an approximate shape:

$$\frac{d\sigma^{i}}{dv} = s_c\ f_c\ v^{-1} \tag{22}$$

$$\frac{d\sigma^{el}}{dv} = s_l\ f_c\ v^{-1} \tag{23}$$

where:

$$f_c = \frac{2\ \pi\ Z_P}{|v - v_1|}\left[1 - e^{-\frac{2\ \pi\ Z_P}{|v - v_1|}}\right]^{-1} \tag{24}$$

and s_c and s_l are constants which are determined by the projectile charge and target material.

Replacing (22), (23) and (24) in (4), we obtain:

$H(v,x) = f_c\ h(v,x)/(v\ v_x)$

$$h(x) = \left(\gamma\, e^{-\frac{\sigma}{v_1} x} + \beta \right) \tag{25}$$

where:

$$\beta = (s_c\, \sigma^{el} + s_l\, \sigma^{r})/\, \sigma \tag{26}$$

$$\sigma = \sigma^{r} + \sigma^{el} \tag{27}$$

For a neutral initial beam, we háve:

$$\gamma = (s_l - s_c)\, \sigma^{el}/\, \sigma \tag{28}$$

If there are only ions in the incident beam:

$$\gamma = (-s_l + s_c)\, \sigma^{r}/\, \sigma \tag{29}$$

We introduce the function E_c, defined by:

$$v_x \frac{\partial Ec}{\partial x} = f_c \left(\gamma\, e^{-\frac{\sigma}{v_1} x} + \beta \right) /\, v - E_c(v,x)\, \mathcal{P}(v) \tag{30}$$

with: $\mathcal{P}(v) = \sum_f \sigma^{*e}_{0f}(v) + \sigma^{ee}(v)$

This E_c approaches the electron distribution for $v \in [v_1 - \delta, v_1 + \delta]$, where δ defines a small range, and gives the convoy electron distribution. The solution of this equation is:

$$E_c(v,x) = f_c \left(T + B\, e^{-\frac{\mathcal{P}(v)}{v_x} x} + C\, e^{-\frac{\sigma}{v_1} x} \right) /\, v \tag{31}$$

$$T = \frac{\beta}{\mathcal{P}(v)}$$

$$C = \frac{v_1 \, \gamma}{(\mathcal{P}(v) \, v_1 - \sigma \, v_x)} \tag{32}$$

$$B = - (T + C)$$

where we choose x=0 as the entrance surface of the ion beam.

The available data for electron excitation of C atoms only consider seven transitions, however the remaining exitation transitions could not be neglected . We assume as a first order approximation, that these transitions may be taken into account by an arbitrary factor that multiplies the theoretical value of σ^{*e}_{0f}, which is calculated from (21), with the values for a_f and b_f described above.

The values for the total cross sections and for the constants s_c and s_l are deduced from a fit to the Koschar et al[11] experimental data of H^0 and H^+ (3 MeV) with the function E_c (31). They are:

σ_c = 3.E-21 cm^2/at [11]; σ_l = 14.1E-18 cm^2/at [11]

α^K_c = .024 [11] α^k_l = .097 [11]

$s_c = L \, \alpha^K_c \, \sigma^r$ $s_l = L \, \alpha^K_l \, \sigma^{el}$

$L = 6$

$\lambda_e = 1/\sigma_e(v_1) = 100$ Å. $\lambda_1 = 1/\sum_f \sigma^{*e}_{0f}(v_1) = 6$ Å.

$\lambda_c = 1/\mathcal{P}(v) = 6.2$ Å.

To obtain the L value we consider the experimental convoy electron yied at $x \longrightarrow \infty$[11], $Y_\infty = T$.

In Fig.3 we graph the function E_c (31) with the above coefficients, it describes the absolute number of the intrinsic convoy electron (ICE) yield, the experimental points correspond to reference [11].

Now, we solve (18) using the finite difference method. We study the electron emission in the forward direction, ie, $\theta = 0$. In that case the elastic gain can be neglected since there is a small probability that the elastic collision of the electronic beam with the background atoms adds particles to that beam.

With that method the electron distribution function reads:

$$F_e(v,x_j) = \left[\frac{(\gamma e^{-\frac{\sigma}{v_i}x} + \beta)\,2\pi}{|v-v_i|(1-\exp(2\pi/|v-v_i|)} - v\,\mathcal{P}(v)F_e(v,x_{j-1}) + \right.$$

$$\left. + \sum_h F_e(v+\Delta E^h_{fi}/v, x_{j-1})\,\sigma^{*e}_h(v+\Delta E^h_{fi}/v)\,(v+\Delta E^h_{fi}/v)\right]$$

$$\times \frac{\Delta x}{v} + F_e(v,x_{j-1}) \qquad (33)$$

The numerical calculation of this equation must omit a neighborhood of the divergent point $v = v_i$. Inside the range $v_i - \delta < v_i < v_i + \delta$ we suppose that the distribution function is well described by the E_c function (31).

That is:

$$f_e(v,x) = \begin{cases} \alpha(\varepsilon)F_e(v,x) & v < v_i - \delta;\ v > v_i + \delta \\ E_c(v,x) & v_i - \delta < v < v_i + \delta \end{cases} \qquad (34)$$

To determine the $\alpha(\delta)$ factor we study the electronic density evolution. We start from (18), neglecting elastic gain and making the integration in velocity:

$$\int v \frac{\partial f_e}{\partial x} dv = \int dv \Big[H(v,x) - f_e(v,x)\ v\ (\sum_h \sigma_{0f}^{*e}(v) + \sigma^{ee}(v)) +$$

$$\sum_f f_e((v^2+ 2\Delta E_{f1})^{1/2}, \theta, x)\ \sigma_f^{*e}((v^2+ 2\Delta E_{f1})^{1/2})\ (v^2+ 2\Delta E_{f1})^{1/2}\Big]$$

Substituting here the solution (34) it is possible to obtain the equation for $\alpha(\varepsilon)$:

$$\alpha(\varepsilon) = \frac{\int_0^\infty dv(H(v,x) - \mathcal{P}(v)E_c(v,x) - v\ \partial E_c(v,x)/\partial x)}{\int'(v\partial F_e(v,x)/\partial x + \mathcal{P}(v)F_e(v,x) + G(v)F_e(v))dv} = 1$$

with $\int' = \int_0^{v-\delta} + \int_{v+\delta}^\infty$

In the Figs. 4-6 we show the calculated electron distribution function for the collision of H^0, at 3 MeV, with carbon-foils of different thicknesses. For comparison with the experiment the distribution must be convoluted with the angular and momentum resolution of the equipment. We make this convolution using the method of Dettmann[2], considering an angular resolution of $.1^\circ$ and a momentum resolution of .7 %. The result is shown in Fig.7. A good agreement with the experimental results is observed.

When the foil is sufficiently thin, only the known convoy electron peak is observed (Fig.4); meanwhile when the target thickness increases, a second structure begins to appear, which shifts to the region of lower velocities (Fig.5). This structure is caused by the convoy electrons produced inside the solid, by electron loss or capture prosseses, which loose their initial energy by inelastic collision furthermore they are elastically scattered by the target atoms. When the foil-thickness is sufficiently large the number of collisions is so high that the scattered electrons may be thermalized. Then they only contribute to the low energy electrons spectrum. In that case again only the convoy structure appear, but with a much smaller intensity (Fig.6).

It is very interesting to note the good qualitative accord between the form of the not convoy electron (NCE) spectrum, described by Yamazaki[20] and our calculations. The NCE are characterized by the function F_e. It is graphed in the Fig. 8.

Now we are interested in the analysis of the relation between the evolution of the intrinsic convoy electrons (IEC), characterized by the function E_c, with the other, or "background" electrons (BE). We define the BE distribution function as:

$$N(v,x) = f_e(v,x) - E_c(v,x) \tag{35}$$

In Fig. 9 we represent, for different target thicknesses, the ratio $E_c(v_1-\varepsilon,x)/N(v_1-\varepsilon,x)$. It is observed that this ratio is constant when the thickness is larger than a certain value.

In Fig. 10-12 we describe the collision of H^+ with C - foil of differents thicknesses. When the target thickness is increased, we observe that the second displaced structure mentioned above, appear again. It is also produced by the collision of convoy electron with the target atoms. Because the absence of direct electron loss to continuum in H^{+} + C collision, the ICE yield for H^{+} never decrease, then the displaced structure has not a maximum (Fig 11). Upon further increase of thickness the peak form does not change any more (Fig. 12). Note that, for a sufficiently thick C foil, the electron spectrum is almost equal for H^{0} or H^{+} beams (Figs. 6 and 12).

CONCLUSIONS

In this paper it has been possible, using a transport theory, to describe the experimentally observed structure of electron spectra obtained when H^{0} and H^{+} colide with C foils of different thicknesses.

Starting from a generalized Boltzmann equation, and considering that the differential cross section of electron loss and ionization, are mainly determined by the Coulomb factor, we study the H^{0}- C foil collision. We describe, in good cualitative accord with the experiment, the electron spectrum for different target thicknesses. Studing the collision of H^{+} with carbon foil, we observe that, when the target thicknesses increase, the displaced structure appair again, but it is less pronounced and has not a maximum. This effect has not been experimentally reported yet. The peak form does not change, if the thickness continues to grow.

Furthermore, with this model of production of convoy electrons inside the solid, we obtain the same constant behaviour of the ratio between the ICE and BE which has been observed by Yamazaki and Oda[11]. We think that it is possible to describe this ratio because the electron distribution function are deduced starting from a generalized transport equation, which considers all the process in one and the same equation. Therefore it is not necessary introduce ad-hoc a Landau function[11-13] which describe the inelastic processes.

In the present model we calculate the parameters in such form that the ICE yield could describe the experimental data. We know that the value considered for the elastic mean free path λ_e is greather than that corresponding to free electrons. In part, this is so, because in our model, we neglected the elastic gain at zero degree, then the elastic losses are overvalued.

Note also, that the comparison with the experiment would be better if the value for the inelastic mean free path, λ_i, is less than the free electrons ones. This may be understood if we take into account the interaction of the convoy electron with the projectil. It would be in accordance with the concept of Coulomb defocussing. In particular, in the Fig.7 of reference [25], it is observed that the convoy electron population is depleted rapidly, in a collection volumen which cover the longitudinal interval $v_i \pm .25$ and a transversal width $v_T=.25$, in comparison with the free electron population. It is due to a single collision sufficies in most cases to remove an electron from the collection volumen, because of the relative large energy transfer per collision[25].

The total mean free path λ_c is mainly determinted by the λ_i. For incident H^0_i, λ_c determines the target thicknesses for which the ICE yield reaches the maximum value, this maximum position is independent of the value of L (Fig. 13). It would be interesting to make a new experiment to determine this total mean free path.

For this purpose, the maximun of the ICE yield would have to be measured with H^0 on dense gases at velocities $v_1 \cong 1$ or 2 a.u. or on C foils with beam velocities $v_1 >> 10$ a.u.. Experiments like these have already been proposed but not performed yet, very likelybecause of the experimental difficulties. Therefore, we propose a re-examination of the intermedium thicknesses in order to obtain the inflection point of the ICE yield. Like the maximum point, the inflection point is also directly related to λ_c.

A determination of λ_c in this way, would shed some light on the effect of the projectile when the transport of convoy electrons in the solid is studied.

All the results descrived above could be improved if we consider the contribution from ionization of the atoms at rest, by electron impact. Nevertheless, a completely different method exists to evaluate the energy loss of electrons interacting with solids. It is connected with the dielectric properties of the material, and it has been succesfully employed in calculations of energy loss distribution for electrons transmitted through thin layer of carbon[21,22,23]. The dielectric description of slowing down may be considered as an alternative to the Bethe deduction of cross section[24].

ACKNOWLEDGEMENT

We would like to thank Dr. W. Meckbach and Dr. R. Barrachina for helpful comments.

REFERENCES

1. W.Meckbach and P.Focke, Nucl.Inst.Meth. **B33**, 255 (1988).
2. K.Dettman, K.G.Harrison and M.W.Lucas, J.Phys.B **7**, 269 (1974).
3. V.H.Ponce and W.Meckbach, Comm.At.Mol.Phys. **10**, 231 (1981).
4. V.N.Neelavathi, R.Richie and W.Brandt, Phys.Rev.Lett. **33**, 302 (1974).
5. Y.Yamazaki and N. Oda, Nuc.Inst,Meth. **194**, 415 (1982).
6. R.Latz, G. Aster, H. J. Frischkorn, P. Koschar, J. Pfenning, J. Schader and K.O. Groeneveld, Nucl.Inst.Meth. **194**, 315 (1982).
7. R. Latz, J. Schader, H.J. Frischkorn, K.O. Groeneveld, D. Hofmann and P. Koschar, Z.Phys.A **304**, 367 (1982).
8. R. Latz, J. Schader, H.J. Frischkorn, P. Koschar, D. Hofmann, K.O. Groeneveld and W. Meckbach, Nucl.Inst.Meth. **B2**, 265 (1984).
9. H.P. Hülskötter, J, Burdöfer, I.A. Sellin, Nucl.Inst.Meth. **B24/25**, 147 (1987).
10. P. Koschar, G. Szabó, A. Clouvas, J. Kemmler, O. Heil, C. Biedermann, H. Rothard, K. Kroneberger, S. Lencinas and K.O. Groeneveld, Journal de Physique C **9**, 275 (1987).
11. P. Koschar, A. Clouvas, O. Heil, M. Burkhard, J. Kemmler and K.O. Groeneveld, Nucl.Inst.Meth. **B24/25**, 153, (1987).
12. Y. Yamazaki and N. Oda, Phys.Rev.Lett. **52**, 29 (1984).
13. R.O. Barrachina, A. Goñi, P. Focke, and W. Meckbach, Nucl. Inst. Meth. **B33**,330, (1988).
14. M.L. Martiarena and C.R. Garibotti, Physica A **166**, 115 (1990).
15. S.K.Allison, Rev.Mod.Phys. **30**, 1137 (1958).
16. N.P. Kalashnikov, V.S. Remizovich and M.I. Ryazanov,

"Collisions of Fast Charged Particles in Solids", Gordon and Breach Science Publishers, Amsterdam, (1985).

17. Mott and Massey, "The Theory of Atomic Collisions", Oxford University Press, (1965).
18. M. Inokuti, Rev.Mod.Phys. **43**, 297 (1971).
19. P. Ganas, Physica **104C**, 411 (1981).
20. Y. Yamazaki, "High-Energy Ion-Atom Collision", Lecture Notes in Physics, vol. 294, 321, Springer - Verlag, Berlin, (1988).
21. J.C. Ashley, J.J. Cowan, R.H. Ritchie, V.E. Anderson and J. Hoelzl, Thin Solid Films **60**, 361 (1971).
22. J. Kemmler, S. Lencinas, P. Koschar, O. Hiel, H. Rothard, K. Kroneberg, Gy. Szabo and K.O. Groeneveld, Nucl.Inst. Meth. **B33**, 317 (1988).
23. S. Lencinas, J. Burgdöfer, J. Kemmler, O. Hiel, K. Kroneberger, H. Rothard and K.O. Groeneveld, Phys. Rev. A **41**, 1435 (1990).
24. E. Bonderup, "Penetration of Charged Particules through Matter, Univ. of Aarhus, Denmark, (1974).
25. J. Burgdörfer, "High-Energy Ion-Atom Collision", Lecture Notes in Physics, vol. 294, 344, Springer - Verlag, Berlin, (1988).

FIGURE CAPTIONS

Fig. 1. Three dimensional plot of logarithmic absolute numbers of electrons emitted under 0° from carbon foils after H^0 and H^+ (3MeV) impact as a function of the logarithmic target thickness ρx. [11]

Fig. 2. (a) The ICE peak height; (b) the ratio of ICE peak height to the BE intensity at the ICE peak energy, I_{ICE}/I_{BE}; and (c) the modified ratio, $v_i I_{ICE}/I_{BE}$, as functions of dwell time. [12]

Fig. 3. ICE yield per incident projectile of H^0 (full circle[11]): —·— present model; —— reference [11]; and H^+ (open square) :—··— present model; – – reference [11].

Fig. 4. Logarithmic convoluted electron distribution considering an angular resolution of $.1^{\circ}$ and a momentum resolution of .7% of H^0 (3MeV) traversing a carbon foil of ρx = .71 μg/cm as function of electron velocity.

Fig. 5. Idem Fig. 4 for ρx = 4.98 μg/cm^2.

Fig. 6. Idem Fig. 4 for ρx = 26.12 μg/cm^2.

Fig. 7. Comparison of the convoluted electron distribution of H^0 (3MeV) traversing a carbon foil of ρx = 9.03 μg/cm descrived by the present model with the experimental curve

of the reference [11]. ——, with λ_c = 6.2 Å, L = 6 ; — — with λ_c = 8.6 Å, L = 4; and ---- with λ_c = 16.4 Å, L = 1.9.

Fig.8. BE distribution H^0 (3MeV) traversing a carbon foil of ρx = 9.03 μg/cm as function of electron velocity.

Fig.9. The ratio of ICE peak height to the BE intensity at the ICE peak velocity, ICE/BE, as function of target thicknesses [μg/cm^2]. The ICE peak is descrived by the function $E_c(v_1 - \varepsilon, x)$ and the BE intensity by $N(v_1 - \varepsilon, x)$ —— H^0 , — — H^+

Fig.10 Logarithmic convoluted electron distribution of H^+ (3MeV) traversing a carbon foil of ρx = .71 μg/cm as function of electron velocity.

Fig.11 Idem Fig.9 for ρx = 4.98 μg/cm^2.

Fig.12 Idem Fig.4 for ρx > 9.03 μg/cm^2.

Fig.13 ICE yield per incident projectile of H^0 (3 MeV) on C foil as a function of target thicknesses [μg/cm^2], for different values of the total mean free path .

—— λ_c = 6.2 Å, L = 6; ---- λ_c = 8.6 Å, L = 4;

— — λ_c = 16.4 Å, L = 1.9.

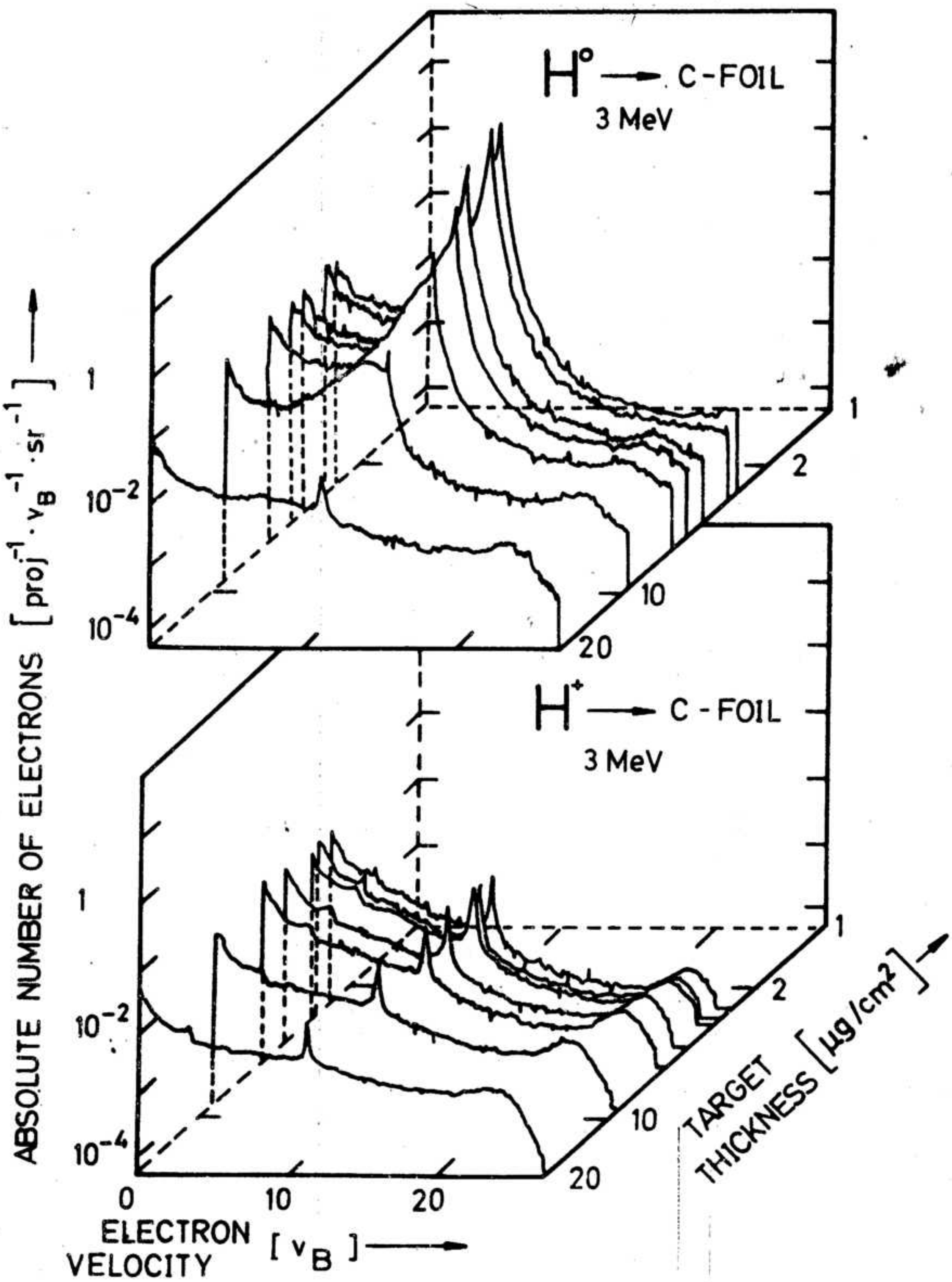

Fig. 1 A. L MARTINEZ et al
PR.A

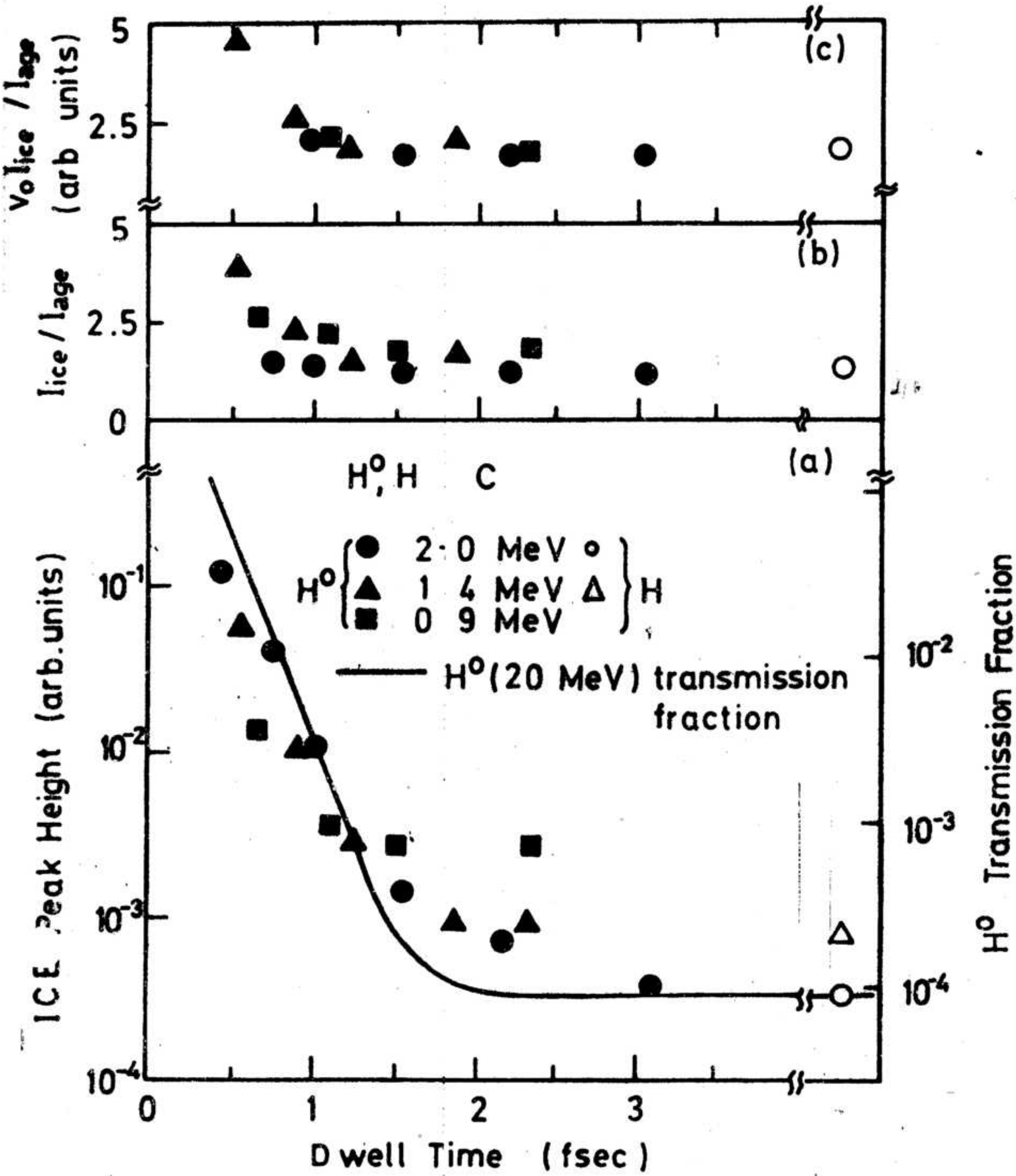

Fig. 2 M.L MARTIARENA

PR A

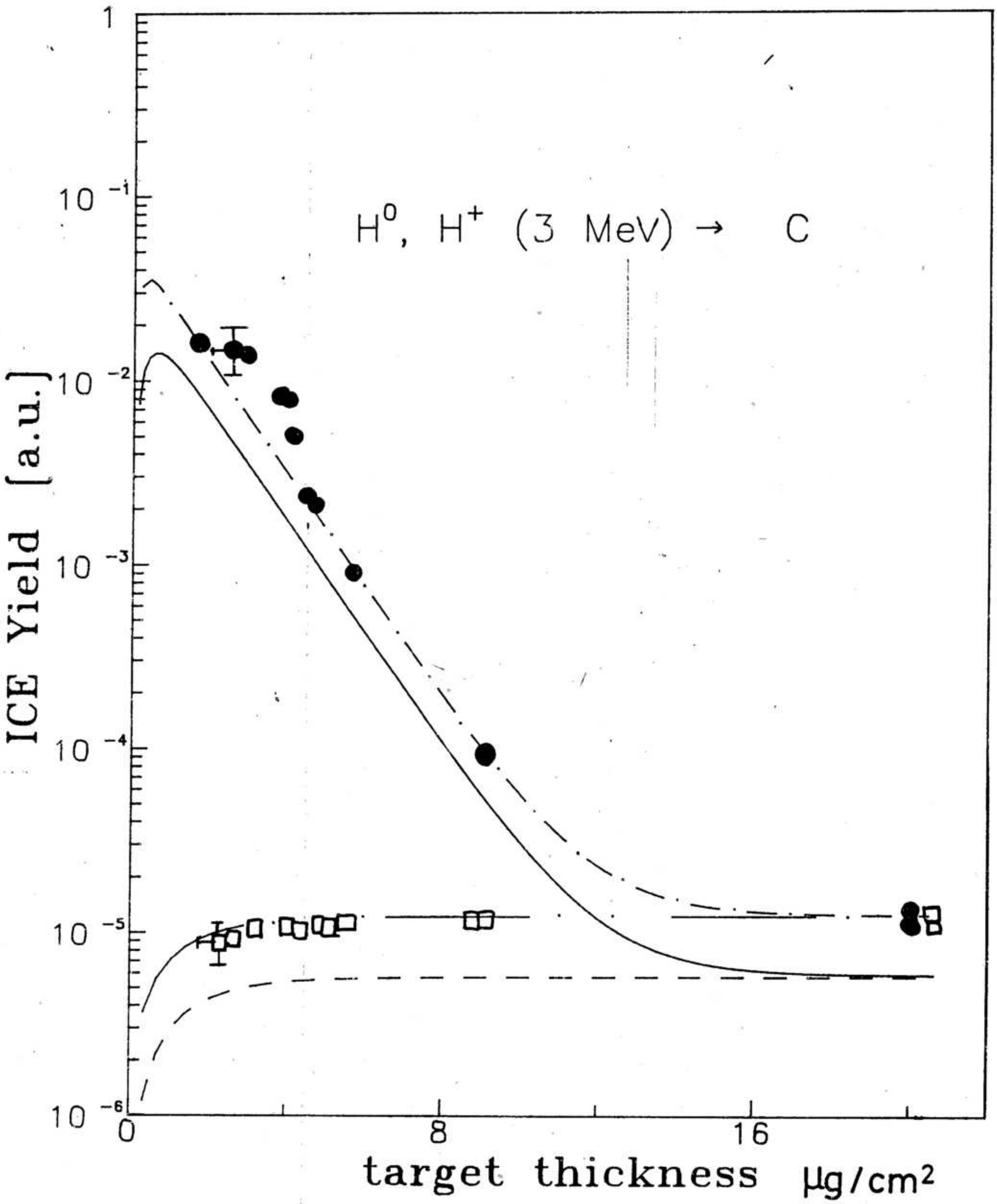

Fig. 3 M. L MARTIARENA
P.R.A

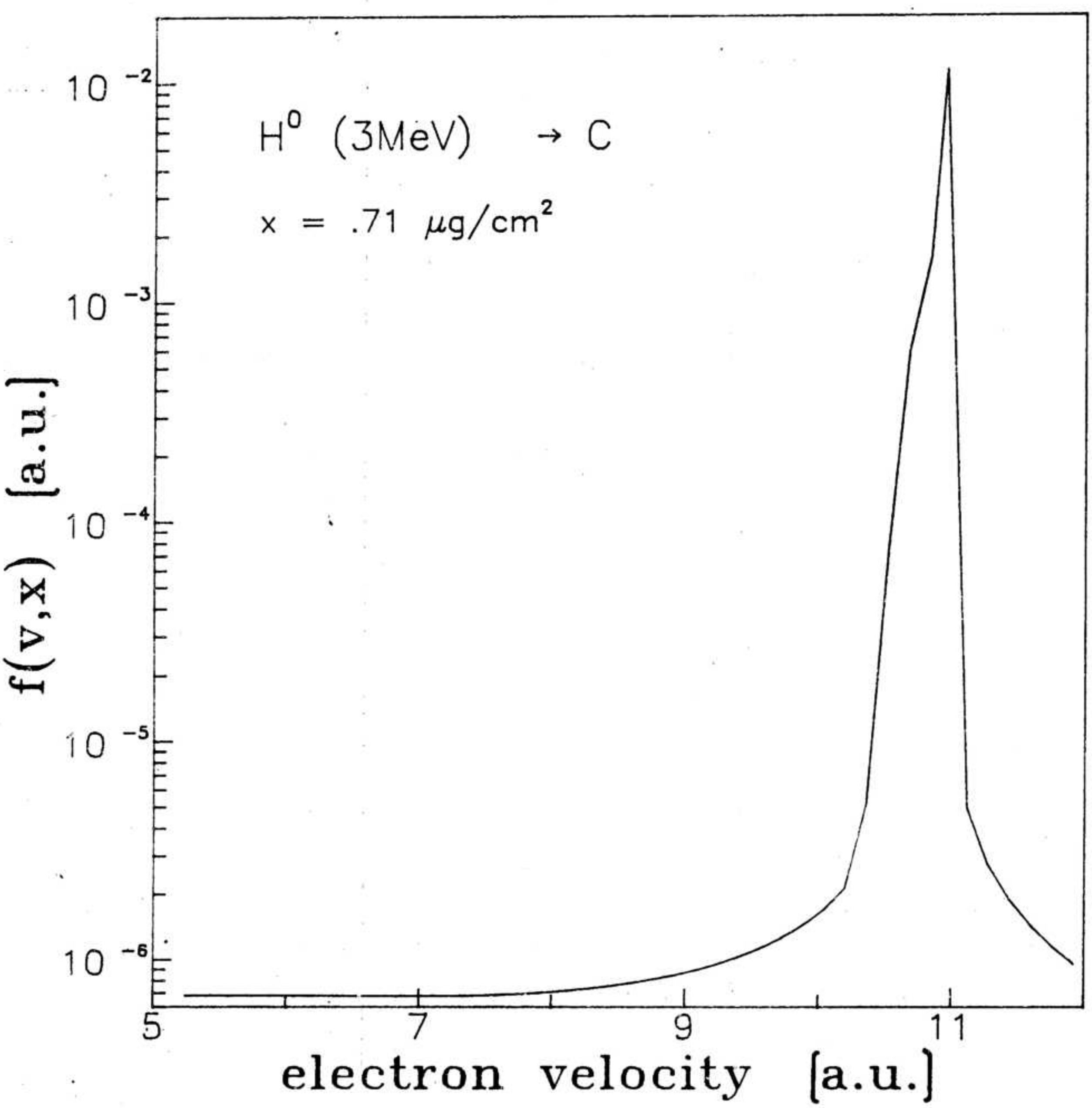

Fig. 4 M. L MARTIARENA

P.R A

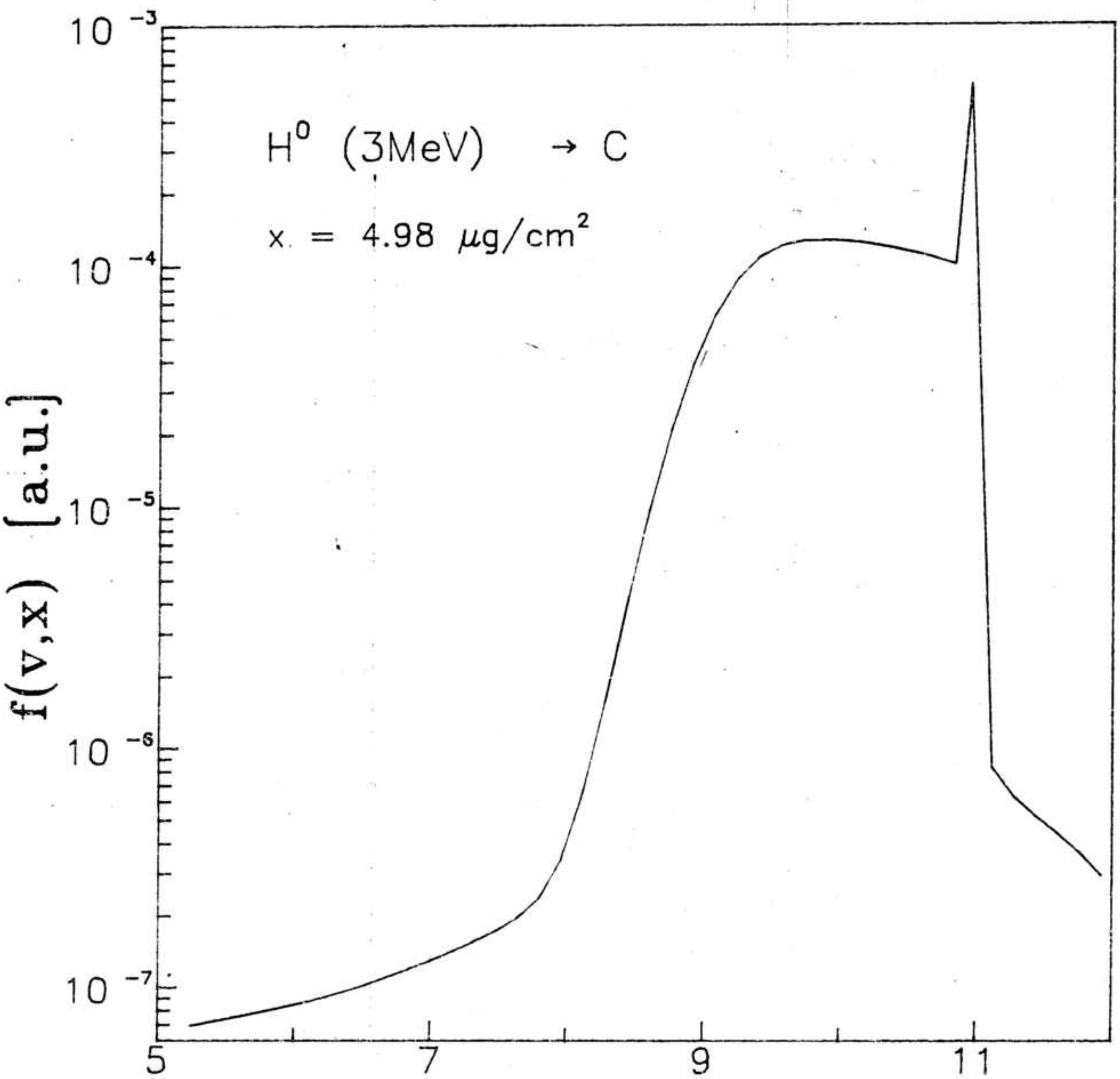

Fig.5 ML MARTIARENA

PR A

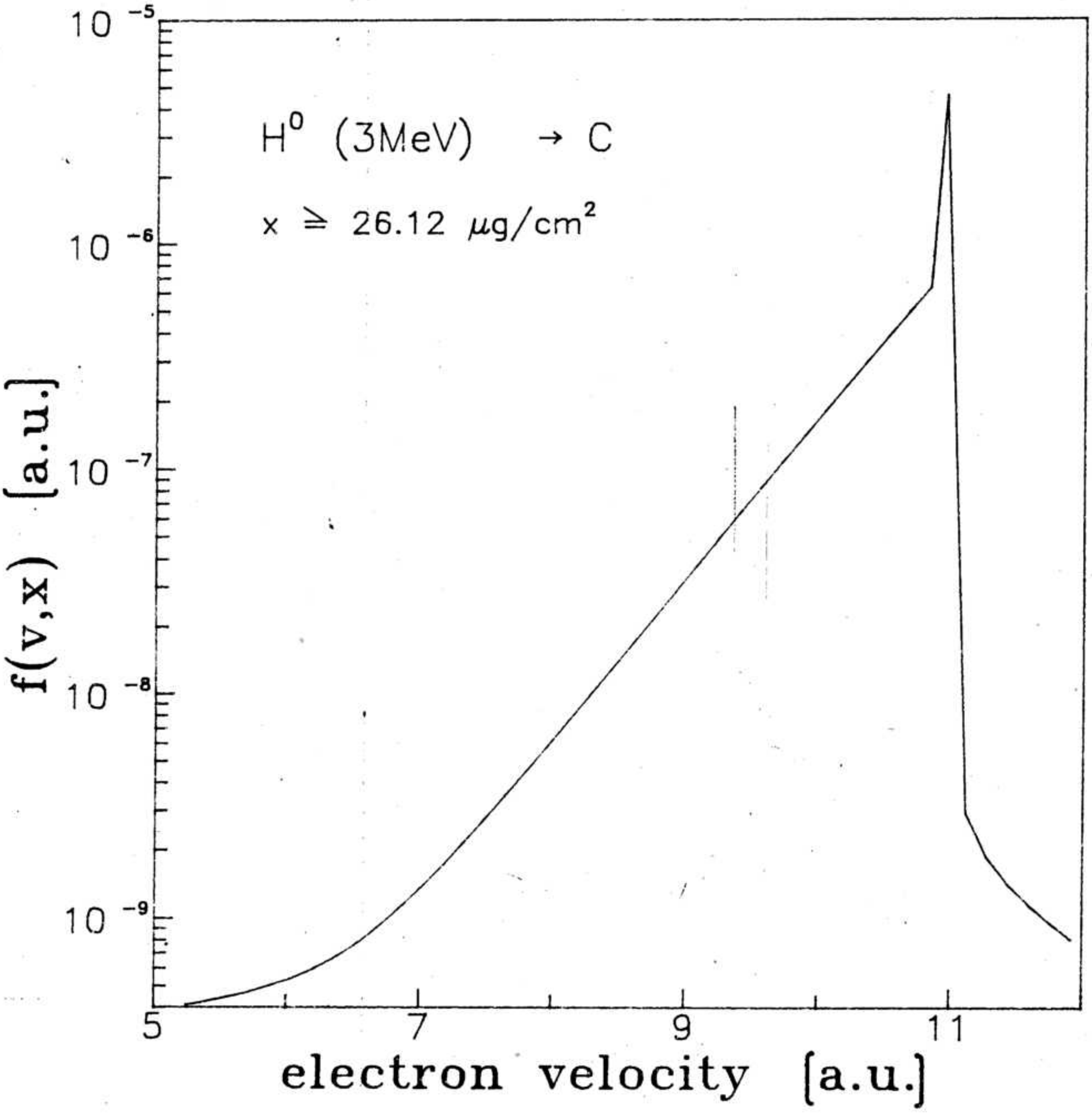

Fig. 6 M. L. MARTIAR...NA

P.R.A

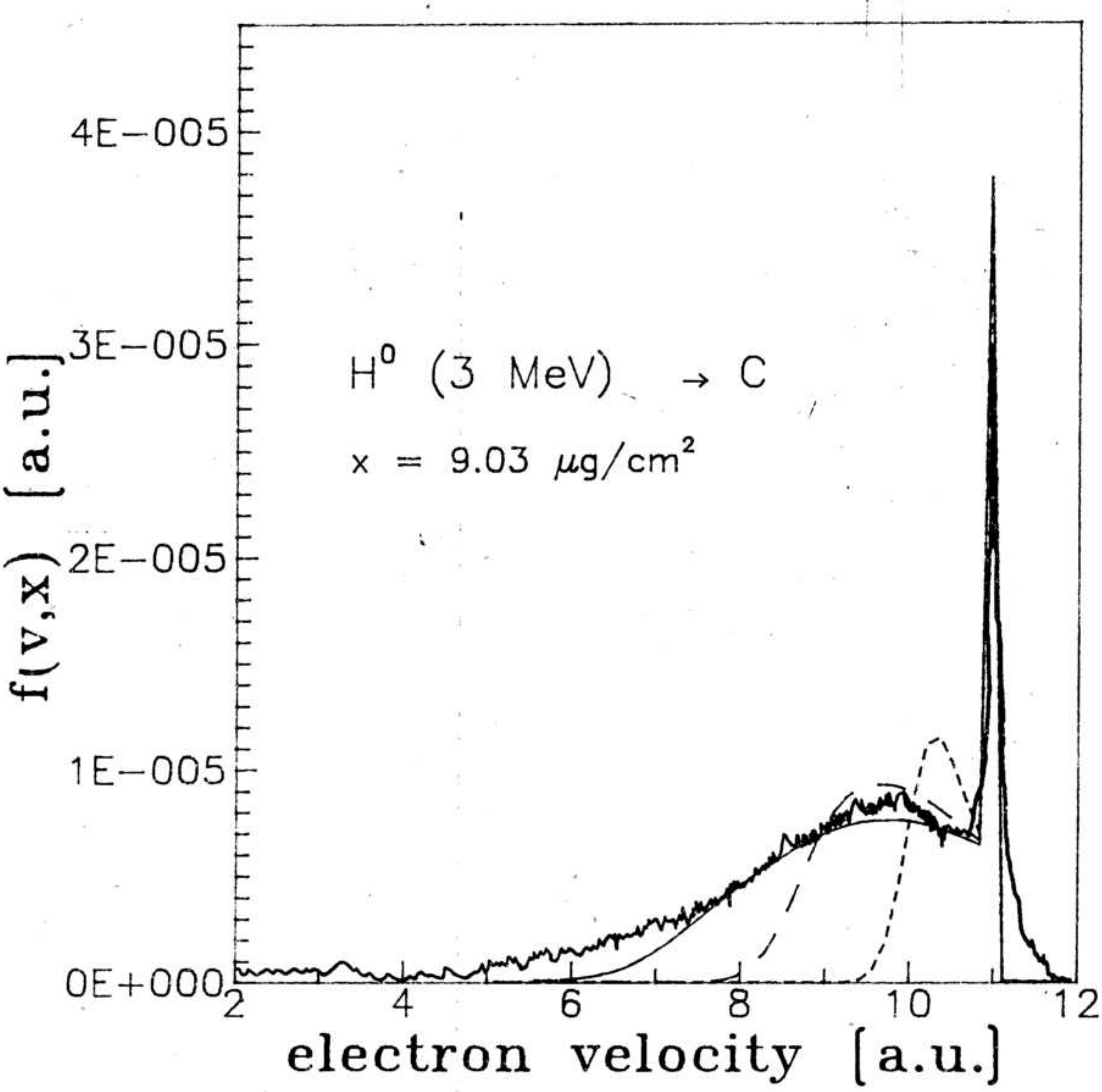

Fig. 7 M. L. MARTIARENA

PR A

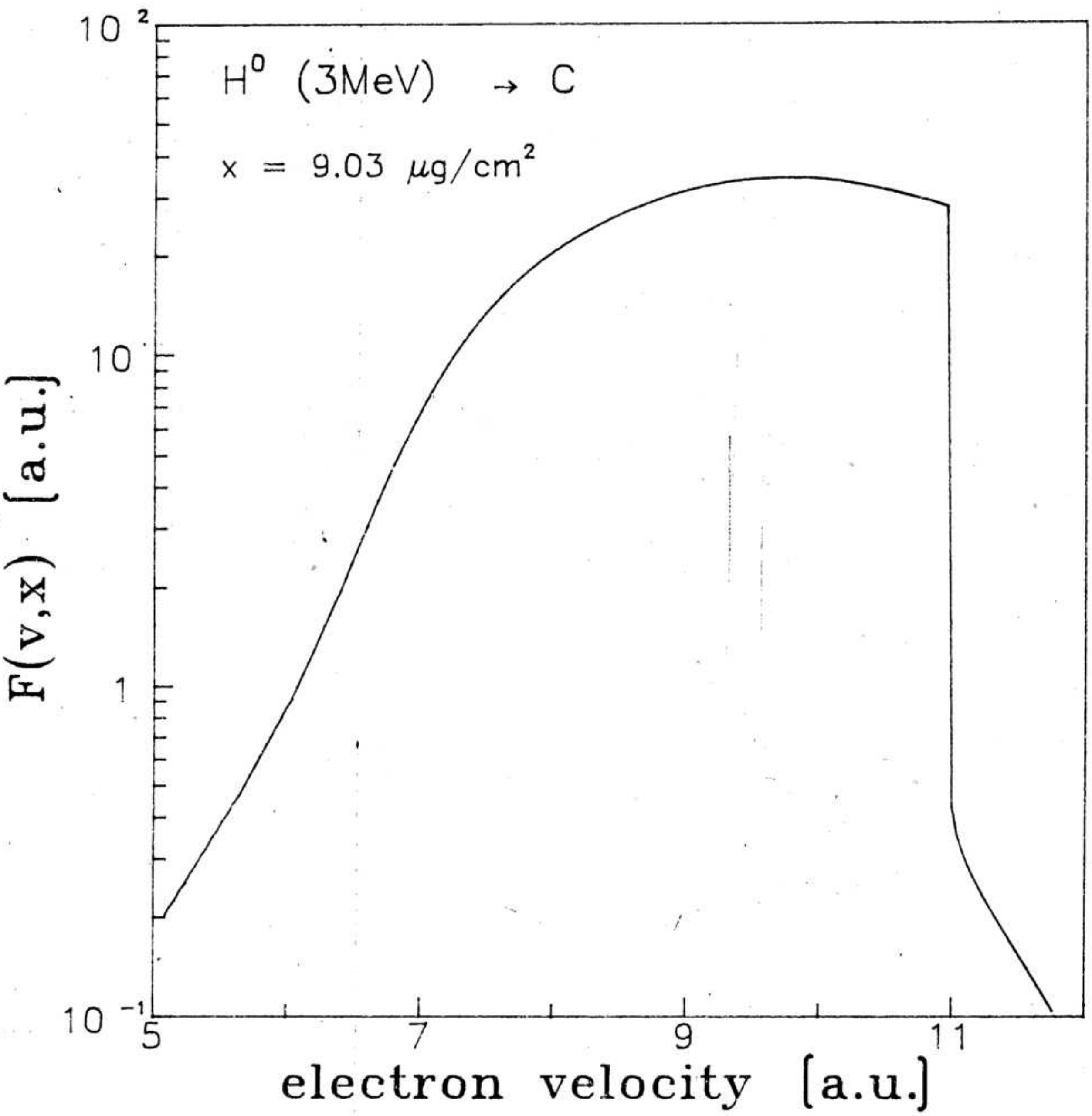

Fig.8 M.L MARTIARENA

P.R. A

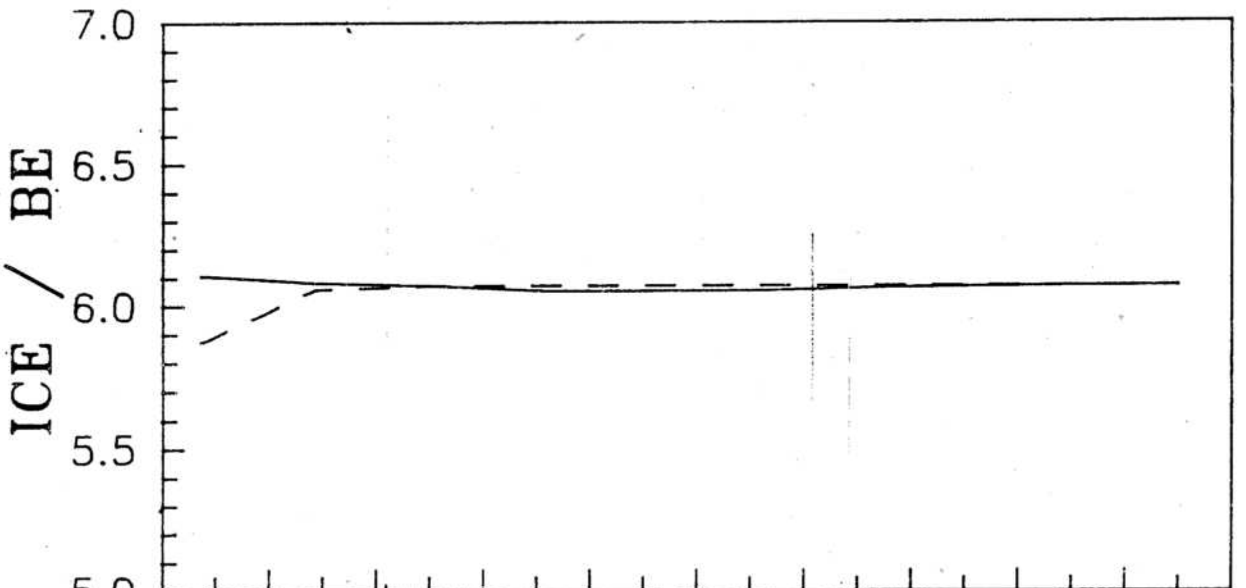

Fig. 9 ML MARTIARENA

P.R.A

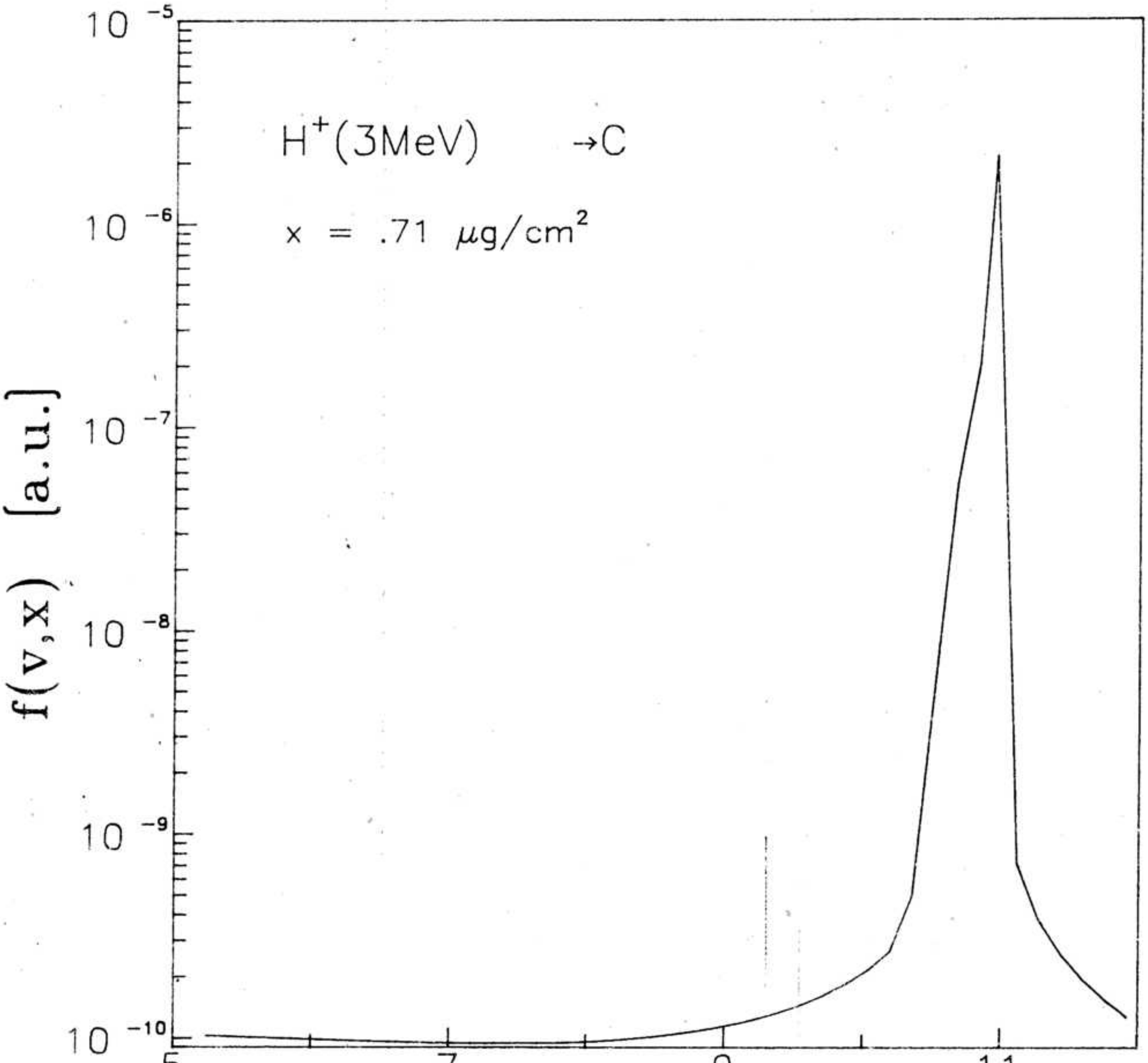

H^+(3MeV) →C
x = .71 μg/cm²
f(v,x) [a.u.]
10^{-5}
10^{-6}
10^{-7}
10^{-8}
10^{-9}
10^{-10}
5
7
9
11
electron velocity [a.u.]

Fig. 10

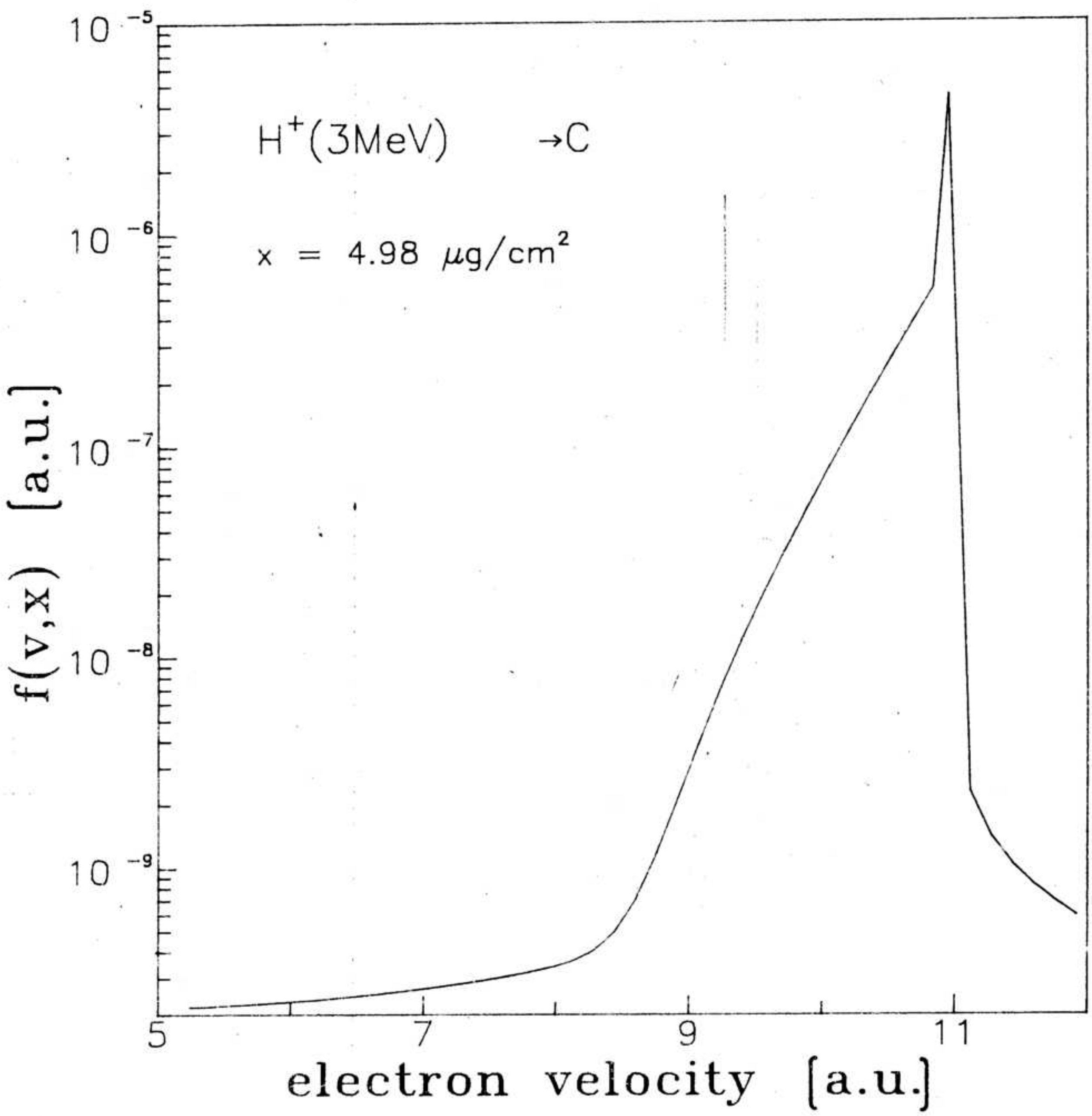
H⁺(3MeV) →C
x = 4.98 μg/cm²
f(v,x) [a.u.]
electron velocity [a.u.]
10⁻⁵
10⁻⁶
10⁻⁷
10⁻⁸
10⁻⁹
5
7
9
11

Fig. 11

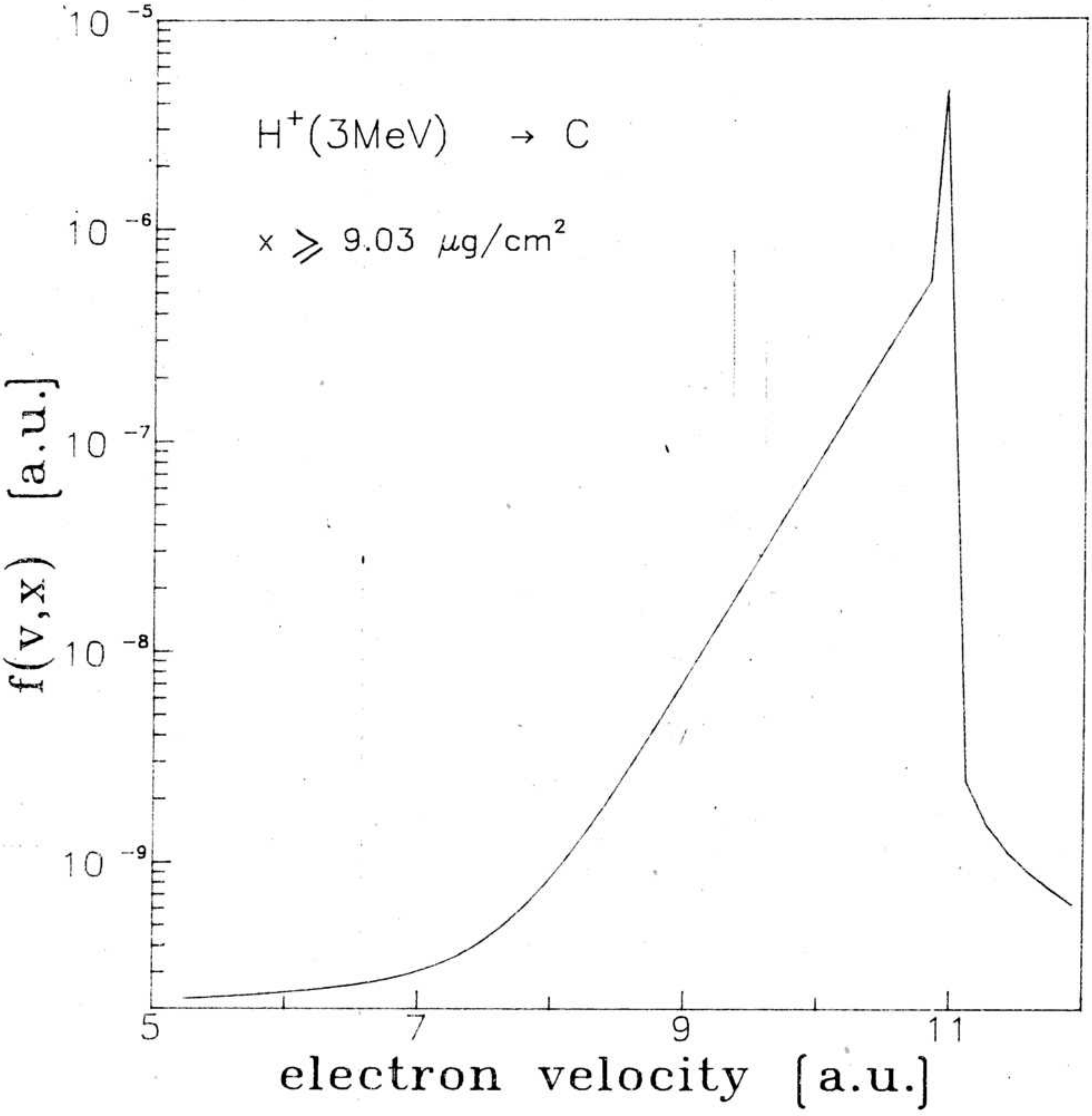

H⁺(3MeV) → C
x ≥ 9.03 μg/cm²
f(v,x) [a.u.]
electron velocity [a.u.]
10⁻⁵
10⁻⁶
10⁻⁷
10⁻⁸
10⁻⁹
5
7
9
11

Fig. 12

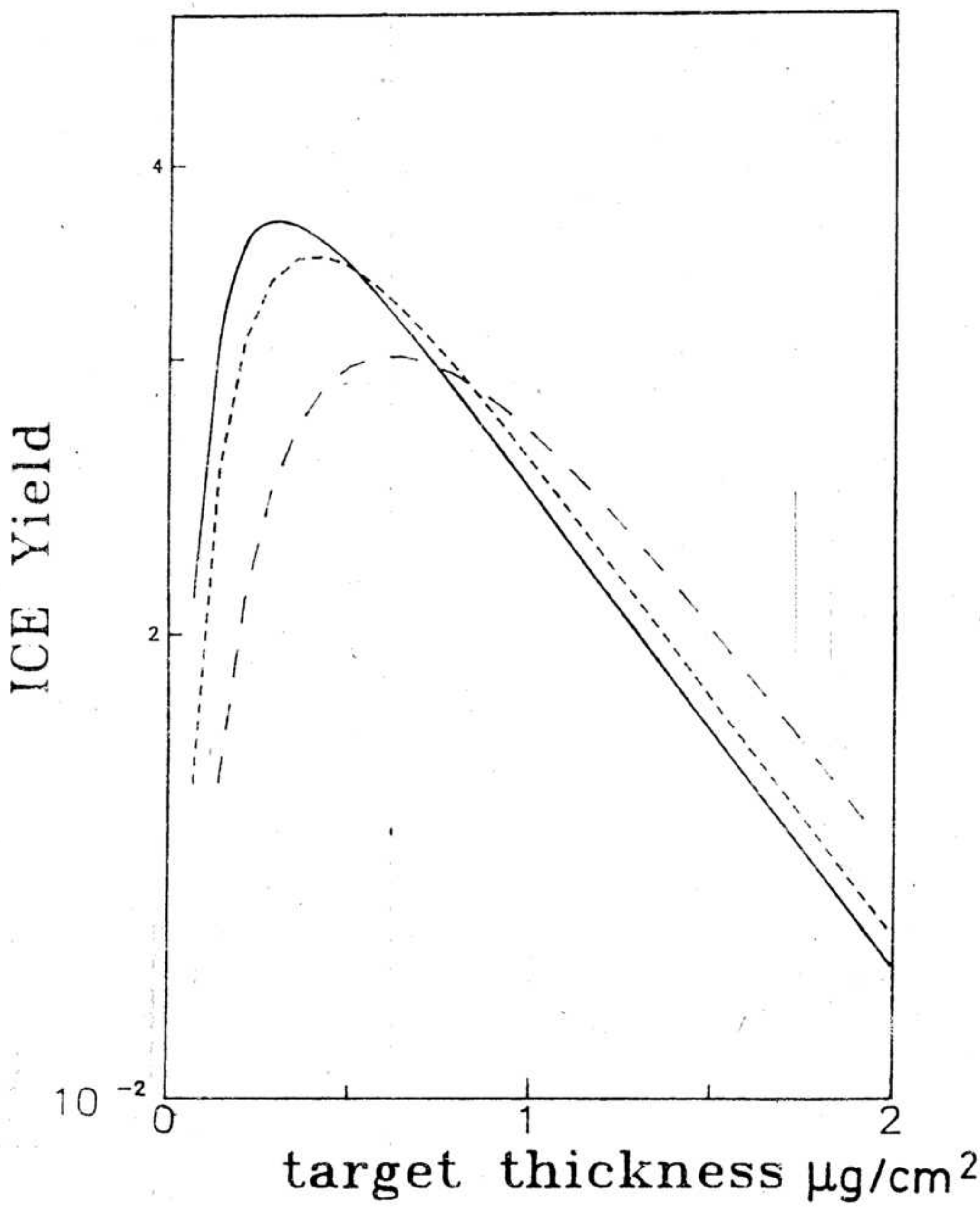
ICE Yield
4
2
10 −2
0
1
2
target thickness μg/cm2